67º congresso 2012 abm
67th abm international congress
ISSN 1516-392X

POWDER INJECTION MOLDING OF NANOSCALE SILICON NITRIDE[1]

Juergen Lenz[2]
Valmikanathan P. Onbattuvelli[2]
Jupiter Palagi de Souza[3]
Ravi K. Enneti[4]
Sundar V. Atre[2]

Abstract
Silicon nitride (Si_3N_4) exhibits many functional properties that are relevant to applications in electronics, aerospace, defense and automotive industries. However, the successful translation of these properties into final applications lies in the net-shaping of ceramics into fully dense microstructures. Increasing the packing density of the starting powders is one effective route to achieve high sintered density and dimensional precision. The present paper presents an in-depth study on the effects of nanoparticle addition on the powder injection molding process (PIM) of Si_3N_4 powder-polymer mixture. Mixing, injection molding, debinding and sintering was successfully demonstrated for a wax-polymer feedstock containing nanoscale Si_3N_4 powders. In addition, feedstock properties were measured and successfully used in Moldflow simulations of an aerospace engine part. The above results provide new design perspectives for PIM of silicon nitride that could impact a wide range of applications.
Key words: Powder injection molding; Nanoparticles; Silicon nitride; Rheology; Engine.

[1] *Technical contribution to 67th ABM International Congress, July, 31th to August 3rd, 2012, Rio de Janeiro, RJ, Brazil.*
[2] *Oregon State University (OSU), USA.*
[3] *Universidade Federal Rio Grande do Sul (UFRGS), Brasil.*
[4] *Global Tungsten Products, Towanda, PA, USA.*

ISSN 1516-392X

1 INTRODUCTION

Silicon nitride (Si_3N_4) has a useful combination of properties including high thermal conductivity, low coefficient of thermal expansion, mechanical strength and chemical stability at elevated temperatures. In order to translate these properties into demanding applications in electronic, energy and transportation sectors, it is necessary to develop net-shaping processes that result in fully dense microstructures.[1]

Among net-shaping techniques, powder injection molding (PIM) is considered to be well-suited for mass production of dimensionally precise, complex part geometries from metals or ceramics (Figure 1). Ceramic powder is compounded with polymers and used to mold parts in an injection molding machine, in a manner analogous to the forming of conventional thermoplastics.[2] The molded part is then subjected to polymer removal (debinding). The debound part is then sintered under controlled time, temperature and atmospheric conditions to get the final part of desired dimensions, density, microstructure and properties. However, the successful application of PIM to Si_3N_4 faces many hurdles. Firstly, defects are possible in the injection-molded components. During debinding, the goal is to remove the polymers in the shortest time with the least impact on the molded part. Additionally, Si_3N_4 cannot be sintered easily due to covalent bonding. Additives are used in such systems to drive the densification by forming a liquid phase.[3,4]

The present paper examines the consequences of nanoparticle addition on the structure, processing and properties of Si_3N_4 by PIM. Further, the feasibility of using the approach for an aerospace engine application was further investigated.

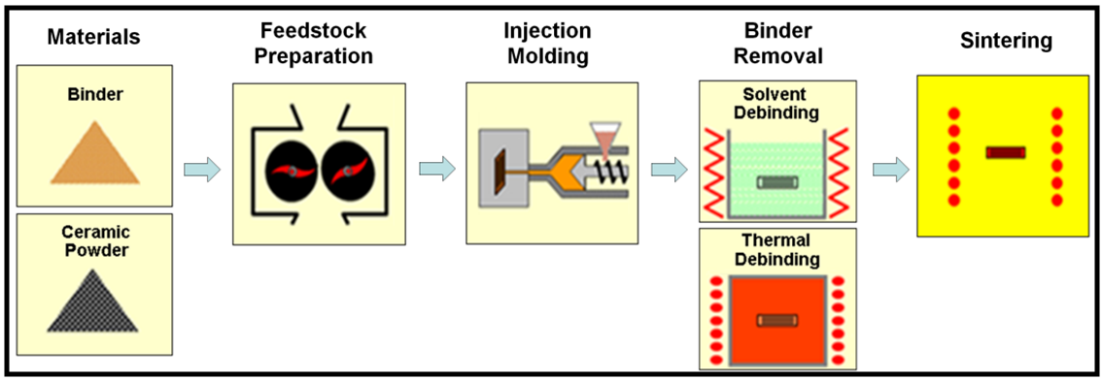

Figure 1. Overview of PIM, showing the flow from powders to the sintered part.

2 MATERIALS AND METHODOLOGY

The starting powder materials contained as-received, commercially available Si_3N_4 with MgO and Y_2O_3 as the sintering additives. A multi-component polymer system based on paraffin wax, polypropylene was chosen as the binder to facilitate a multi-step debinding process. Torque rheometry was performed in the Intelli-Torque Plasticorder (Brabender) in order to determine the maximum packing density of the powder-polymer mixture. Twin screw extrusion of Si_3N_4 feedstocks was performed with an Entek co-rotating 27 mm twin screw extruder with an L/D ratio of 40 and pelletized for further use. Moldflow software was used for simulating the injection conditions. Injection molding was performed on an Arburg 221M injection molding machine. Thermogravimetric analysis (TGA) was performed on the extruded feedstocks using TA-Q500 (TA instruments) thermal system operated under nitrogen

ISSN 1516-392X

flow in the temperature range of 50°C-600°C with a heating rate of 20°C/min. The rheological characteristics of the feedstock were examined on a Gottfert Rheograph 2003 capillary rheometer at different shear rates and temperatures. The testing was carried out in accordance with ASTM D 3835. Powder injection molded Si_3N_4 samples were thermally debound prior to sintering at 1,850°C for 2 h under nitrogen atmosphere. The micrographs of the thermally debound and sintered samples were taken with the QuantaTM–FEG (FEI) dual beam scanning electron microscope (SEM) coupled with an energy dispersive X-ray spectrometer (EDAX). TA Instruments- Q-500 was used to measure the specific heat (C_p) of the sintered samples. Vickers hardness was measured using a Leco microhardness tester.

3 RESULTS AND DISCUSSION

Particle size analysis of the two Si_3N_4 powders used in the study was performed (Figure 2). The median diameters of the two Si_3N_4 powders were found to be 20 nm and 130 nm, respectively and were used in the ratio of 5:95 in the feedstock system.

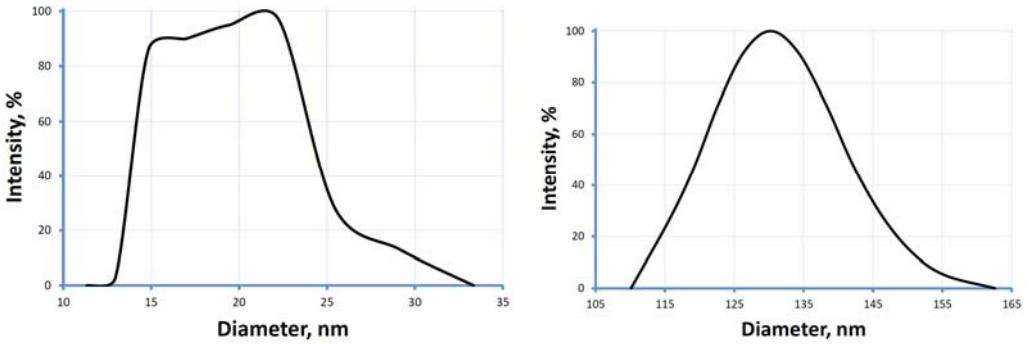

Figure 2. Powder characteristics of the two Si_3N_4 powders used in this study.

The mixing torque is plotted as a function of solids loading in Figure 3 for the Si_3N_4 system. From the figure, it can be noticed mixing torque increases as a function of solids loading. A maximum powder content of 86 wt.% in the powder-binder mixture was achieved with the wax-polymer binder system.

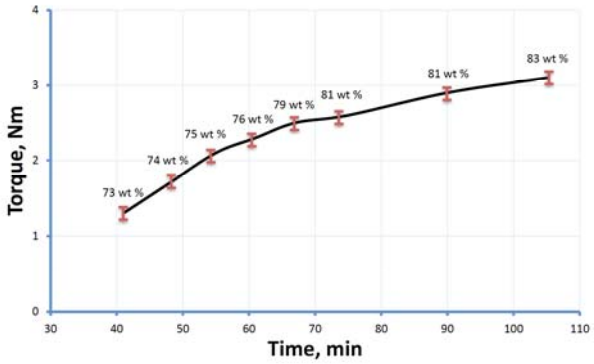

Figure 3. Mixing torque behavior of the Si_3N_4 powder-polymer mixture.

Mixing scale-up was performed on a twin-screw extruder at 80 wt.% powder loading in the feedstock. The Si_3N_4 samples were subject to TGA evaluation to confirm the powder content experimentally. From the TGA plots (Figure 4), the powder content in the Si_3N_4 feedstocks was determined to be 80.07 wt.%.

ISSN 1516-392X

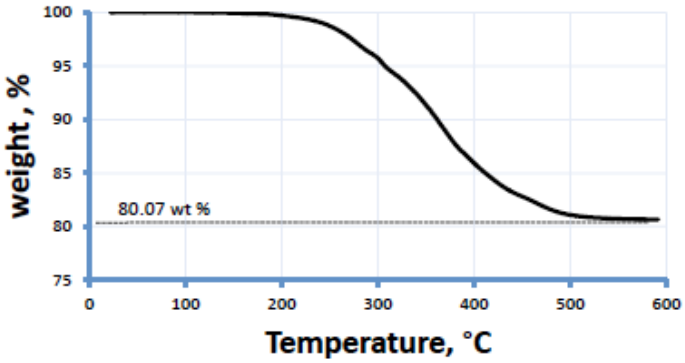

Figure 4. TGA of Si3N4 feedstock.

The apparent viscosity-shear rate curves of Si_3N_4 powder-polymer mixtures were measured at different temperatures (Figure 5). The viscosity of the powder-polymer mixture decreased with an increase in shear rate, indicating pseudoplastic behavior.

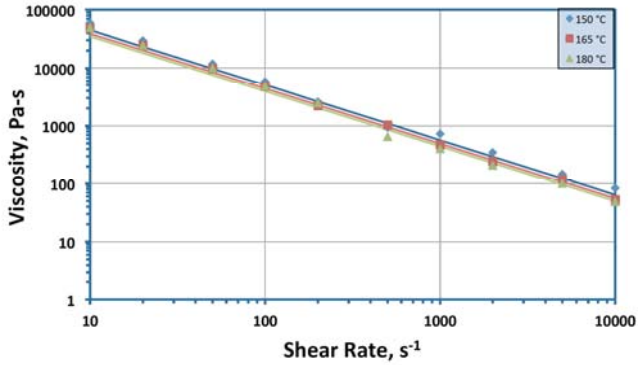

Figure 5. Rheological behavior of Si_3N_4 powder-polymer mixture.

The thermal conductivity and specific heat capacity of the feedstock is shown in Figure 6. In the DSC plot in Figure 6b, peaks were found at ~45°C and ~ 80°C, representing melting points of the wax and polymer constituents, respectively. Additionally, the pressure-volume-temperature (pvT) behavior describing the shrinkage characteristics of the feedstock is shown in Figure 7.

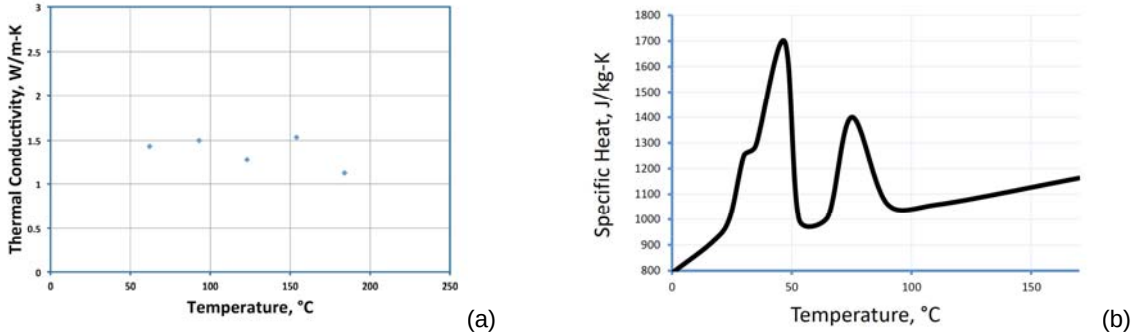

Figure 6. (a) Thermal conductivity; and (b) specific heat capacity of the Si_3N_4 powder-polymer mixture.

ISSN 1516-392X

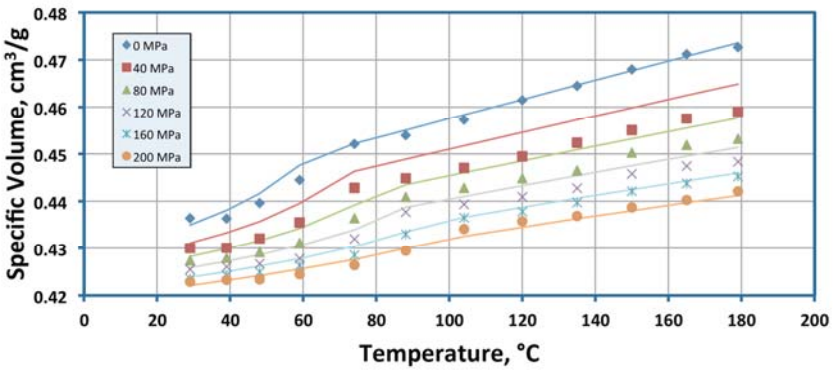

Figure 7. pvT behavior of Si_3N_4 powder-polymer mixture.

Injection molding runs were performed with the Si_3N_4 feedstock to mold a multi-slotted part as shown in the Figure 8. Following debinding, sintering was conducted for the Si_3N_4 samples at Kyocera Corporation. From Figure 8, it can be seen that the densification of Si_3N_4 at 1,850°C resulted in ~15% linear shrinkage. Sintered parts showed a Vickers hardness of 1,200 ± 50 HV1, indicating highly dense parts.

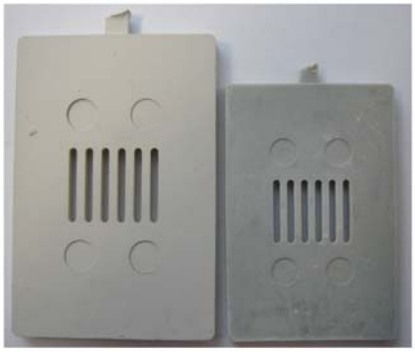

Figure 8. Linear shrinkage from injection molded (left) to sintered (left) Si_3N_4 parts was found to be ~15%.

Figure 9 shows SEM micrographs of Si_3N_4 samples following injection molding and sintering. The surface micrograph of the injection molded parts show an α phase. Following sintering, the specimen microstructures indicate a complete transformation to the β phase. These results indicate that the feedstock composition can be successfully used for injection molding and sintering. Further experiments are needed to optimize sintering conditions to improve microstructures, density, and properties.

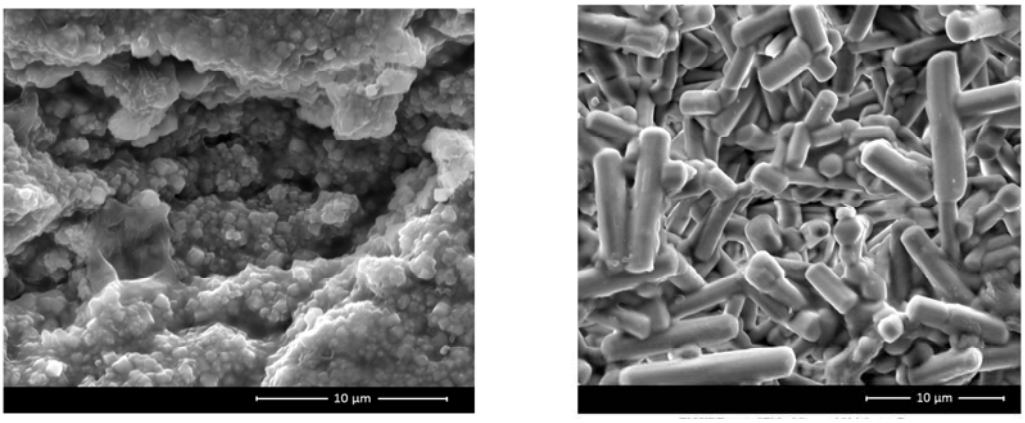

Figure 9. SEM of molded (left) and sintered (right) Si_3N_4 samples.

ISSN 1516-392X

Simulations were performed to evaluate the effects of process conditions and feedstock properties on the mold filling behavior for the slotted geometry (Figure 10). In general, good agreement was found between injection molding experiments and the simulations. These results provided validation of the feedstock property measurements and the simulation platform.

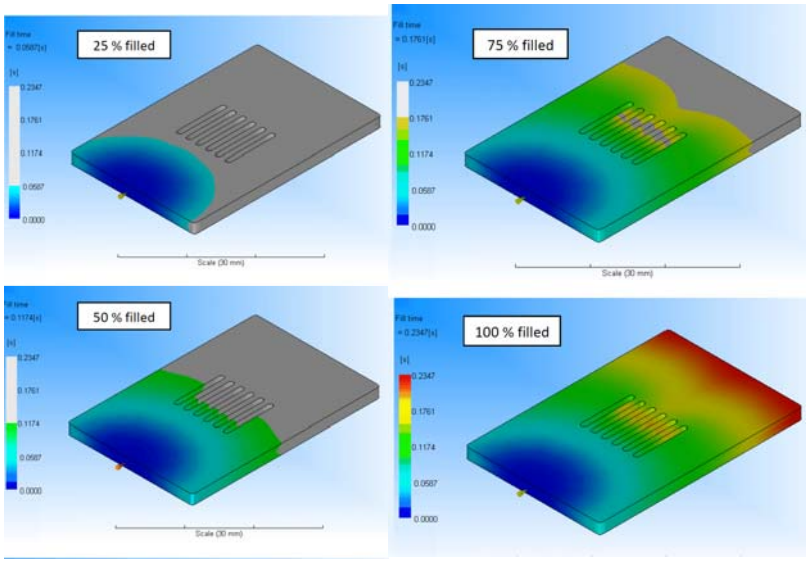

Figure 10. Progressive filling pattern during the injection molding of Si_3N_4 feedstock at 165°C for a slotted geometry used for materials and platform validation.

Based on these results, a more detailed design study was undertaken to extend the design protocol to an engine part used for an aerospace application (Figure 11). A fusion-type finite element mesh was created for this part using the Moldflow software. The mesh had 12,732 triangles and 6,358 connected nodes.

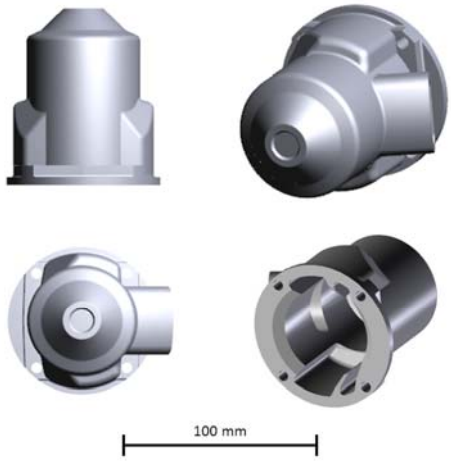

Figure 11. Silicon nitride engine part selected for mold filling simulations**.**

Figure 12 shows the progressive mold fill behavior and the required time to fill the cavity of the engine component using the feedstock properties described earlier. A mold temperature of 28°C and a melt temperature of 165°C was used for this simulation. No significant flow front velocity differences were observed. The part was filled smoothly with no jetting.

ISSN 1516-392X

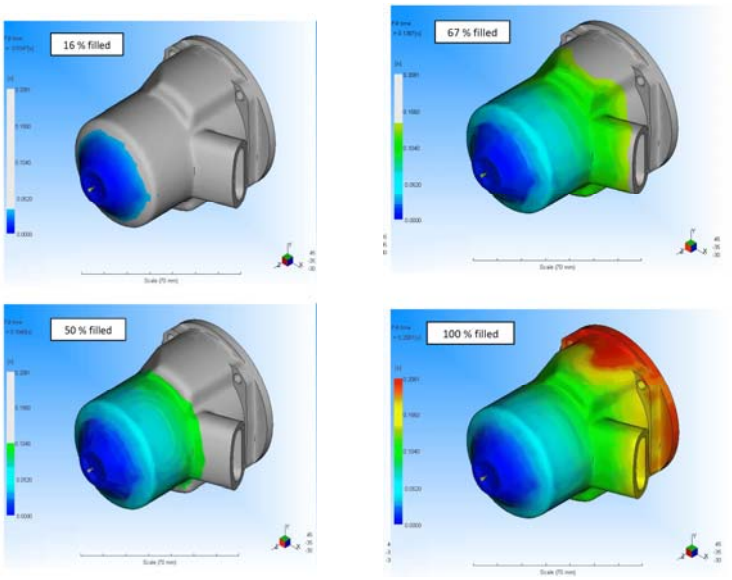

Figure 12. Progressive mold-filling behavior of the silicon nitride engine part at 165°C.

Figure 13a shows the injection pressure distribution in the engine part. The maximum pressure during the simulation was estimated to be 21.67 MPa and occurred at 0.204 sec. This peak was observed right at the injection location. Figure 13b shows the bulk temperature of the flow front. As a general guideline the flow front temperature should not drop more than 2°C to 5°C during the filling phase. If the flow temperature drops more than that, the risk to have a short shot or hesitation is high. In the case of the engine part, the temperature dropped about 0.5°C. Further, no hot spots or cold spots were observed.

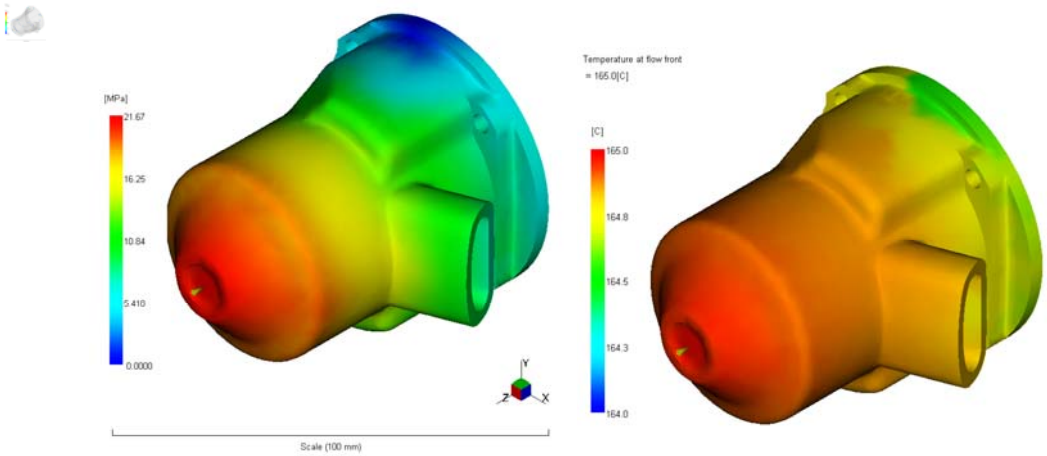

(a) (b)

Figure 13. Injection pressure (left) and bulk temperature (right) distributions in the engine part.

Figure 14a shows the spots where the risks of air traps are located on the engine part. These locations provide a guide for location of vents in the mold cavity to remove surface blemishes. Figure 14b shows where weld lines are likely to occur in the part and also the orientation at which the two flow fronts meet. Weld lines are created when two independent flow fronts travelling in different directions meet. When they bond, the result can be some permanent residuals that can be seen after ejection. In case the two melt fronts where hot enough they merge completely. But if not, two different cases can occur. Either there will be just visual blemishes like a notch or color change on the surface of the part or there could be structural problems

ISSN 1516-392X

as well. In the present study, most of the weld lines were not located in areas of high applied stress and the visual defects were not found to be critical.

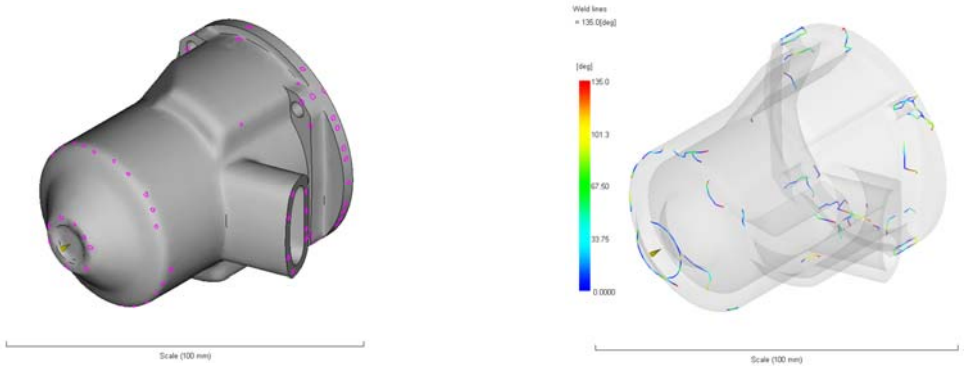

(a) (b)

Figure 14. Air traps (left) and weld lines (right) in the engine component at cubically centered process parameter settings.

4 CONCLUSIONS

This paper presented an in-depth feasibility study on the powder injection molding (PIM) of nanoscale Si_3N_4 powder. The results indicated provided the first demonstration that nanoscale Si_3N_4 could be successfully processed by PIM. In addition, feedstock properties were measured and mold-filling simulations demonstrated that it was feasible to mold the specific engine part with the newly developed nanoscale silicon nitride material system.

REFERENCES

1 R.M. German, A. Bose, Injection Molding of Metal and Ceramics; MPIF, New Jersey, USA, 1997.
2 V.P. Onbattuvelli, S. Vallury, T. McCabe, S-J. Park, S.V. Atre, PIM International, 4(3): 64-70, 2010.
3 R.M. German, Sintering Theory and Practice; John Wiley and Sons Inc, New York, USA, 1996.
4 V.P. Onbattuvelli, S.V. Atre, Review of Net Shape Fabrication of Thermally Conducting Ceramics, Materials and Manufacturing Processes, 26(6):832-845, 2011.